

COVER PAGE

Document downloaded by @DAEL

Sat Nov 21 07:36:14 2026
For personal use

When automatic English translation is provided, only the original document is authentic.
The EAA cannot be held responsible of any translation error

Bibliographical reference

Reduction of Low Frequency Noise Transmitted Through a Single-Pane Window, A.M. Jessop, K.M. Li and J.S. Bolton, Acta Acustica **vol. 97** (Number 3), 2011, pp. 382-390

DOI
https://doi.org/10.3813/AAA.918419

Acta Acustica united with Acustica
Vol. 97 (2011) 382 – 390

DOI 10.3813/AAA.918419

Reduction of Low Frequency Noise Transmitted Through a Single-Pane Window

A. M. Jessop, K. M. Li, J. S. Bolton
Ray W. Herrick Laboratories, School of Mechanical Engineering, Purdue University, 140 S. Martin Jischke Drive, West Lafayette, IN 47907-2031, U.S.A. mmkmli@purdue.edu

Summary
Windows typically comprise the weakest link in sound insulation amongst all the components in a building façade, thus making them good paths for low-frequency noise transmission. Here, the effect on sound transmission of adding non-periodic stiffening elements to windows is explored. The contribution of elastic mounting to low-frequency noise transmission is also considered. A finite element model allowing for both resilient panel mounting and the addition of variable stiffness beams within the panel was constructed. The model allows for variable positioning of beam elements as part of a stiffened panel configuration. Experimental sound transmission loss testing of panels with variable edge stiffness was performed to verify the character of the predictions seen in the models. The results show that the low-frequency sound transmission loss below 150 Hz can be increased by several dB through careful use of stiffening elements, while resilient mounting generally decreases the low-frequency sound transmission loss of windows.

PACS no. 43.40.At, 43.40.Dx, 43.40.Rj

1. Introduction

Sound insulation for mid- to high-frequency noise for residential buildings has been studied widely [1]. However, there is a general increase in low-frequency noise (LFN) in residential and commercial areas that has led to an increased need for building materials that mitigate LFN. Noise spectra from aircraft, cars, and trains have substantial components below 150 Hz, and increased urbanization has brought these sources closer to offices and residences. As the lightest components in a building structure, windows are typically a major transmission path for noise, particularly near their low-frequency resonances. Sound transmission through panels in the very low-frequency region is typically stiffness-controlled and is also dependent on the resonances of the window. In the present study, internal stiffening of windows is studied as a way of mitigating LFN transmission through windows.

Beranek [2] summarized many of the basic equations for sound transmission through single rectangular panels. His analysis divided panel transmission into three distinct regions. Sound transmission in the lowest frequency region is controlled by the stiffness of the panel and its supports and resonances in the panel structure. Sewell [3] and Leppington [4] both incorporated modal vibration into their analytical formulations of sound transmission through panels. They calculated transmission losses of plates as functions of all the modes of the plate that can radiate sound at all frequencies. Leissa [5] comprehensively reviewed analytical and numerical solutions for vibrations of plates restrained by such classical boundary conditions as free, clamped, or simply supported. The determination of the modal resonant frequency of rectangular plates has further been extended to include guided support edges [6]. Further analytical models, developed for double panels with enclosed air cavities, by Xin *et al.* [7] take into account the effect of modes present in the window system and the vibro-acoustic coupling between the window structure and resulting sound transmission.

Work with stiffened plates has typically been conducted in the context of either sandwich panels or periodically stiffened structures, such as those with regular beam spacing or corrugations. Mead [8, 9] considered mode shapes and wave propagation in periodically stiffened plates, and Lee and Kim [10] derived equations to predict sound transmission through periodically stiffened panels. They found that the effect of panel stiffening was significant in raising the transmission loss of the panel at lower frequencies. More recently, Wang *et al.* [11] modeled sound transmission through a periodically-stiffened plate by modeling the plate structure as a single unit having homogenous properties. However, the addition of periodic supports is generally not practical for windows since the addition of numerous stiffening elements may result in unacceptable visual obstruction.

Photiadis [12] studied vibration propagation through fluid-loaded plates with irregularly spaced stiffening elements. He constructed simulations of the stiffened plates

Received 27 June 2010,
accepted 29 January 2011.

© S. Hirzel Verlag · EAA

Document downloaded by @DAEL, 2026-11-21 07:36:17 - personal use only

and tested the results of vibration propagation with fluid coupling, and demonstrated localization of energy in the plate.

Fan [13] explored the effects of elastic damping materials along the borders of a plate. His calculations account for a finite-sized plate with elastic conditions inhibiting translational and rotational motion at its edges. His models show a decrease in transmitted sound levels by as much as 10 dB at the natural frequencies of the lower modes of the plate due to the addition of damping materials at the plate boundary. His calculations were performed in the time-domain and focused on transient vibration decay after the initial excitation thus making them inconvenient for prediction of steady-state transmission loss.

Atalla *et al.* [14] and Berry [15] have explored the high-frequency sound radiation from a thin plate with edges elastically restrained against translation and rotation. The effects of varying boundary support with position on the panel, resulting in shifts in radiated sound power level, were considered.

Sound absorption and damping materials are typically used to reduce the levels of sound transmitted indoors. However, these materials become ineffective for reduction of low frequency noise. The current study exploits the use of a stiffening element to improve the acoustical performance of a single panel at frequencies below 150 Hz. The finite element (FEM) model which was used to examine the feasibility of such an approach for reduction of low frequency noise (LFN) transmitted through a single pane window is described in section 2. Numerical simulations are then presented in section 3 to illustrate the effectiveness of using a single pane window with stiffening elements for reducing the transmission of LFN indoors. An experimental study is presented in section 4 to validate of the numerical model used in the current study. Finally, concluding remarks are offered in section 5.

2. Finite-element modeling

Finite element method (FEM) modeling of panel transmission was performed here to gauge the effects of various structural elements on the transmission of LFN. The current numerical model, shown in Figure 1, is similar to a standing wave tube. Incoming pressure waves were generated in the fluid on one side of the panel and were allowed to propagate away from the panel through the fluid on the other side of the panel. The advantage of using the current FEM scheme is that stiffening elements can be added without changing the geometry of the model. As a result, any changes in the transmission loss of the panel configuration can be attributed to the structural changes in the panel.

The FEM was used to model panels with multiple natural frequencies below 150 Hz. While these models were not explicitly based on actual windows, they represent idealizations useful for identifying trends. The basic, fully-constrained isotropic panel was modified by including single stiffening elements across the panel and by allowing for finite edge stiffness by including elastic mounting elements.

In the FEM models, the panel spanned the full cross-section of a long, rigid-walled tube, and the size of the tube was such that only plane waves propagated at all frequencies considered. As a result, there was no baffling around the panel: the tube and the panel had identical height and width. The panel's edges could be constrained at the wall of the "tube" in a variety of ways without interfering with the incident sound field. Other changes, such as the addition of stiffening elements, could be easily made and adjusted in this model without affecting the plane wave behavior of sound in the tube.

Application of these various boundary conditions on the plate structure and plane-wave requirements in the tube yielded a model consisting of a 1 meter square tube. The anechoic terminations in the tube were located 2 meters from the panel in both directions. The panel was 1 meter square "glass" having a density of 2180 kg/m^3 and a thickness of 2.5 mm. A Young's modulus E of $6.8 \cdot 10^{10}$ N/m^2 and a Poisson's ratio ν of 0.19 were assumed for the glass in the numerical simulations described below.

Numerical simulations were conducted from 1 Hz to 150 Hz in 1 Hz increments. The harmonic analysis mode was used in ANSYS, thus representing steady-state oscillation for plane wave transmission. Post-processing of the FEM model yields the transmission loss of the panel.

In the current model, a technique known as the four-microphone standing wave tube measurement [16] was adopted to determine the transmission loss of the panel.

As shown in Figure 1, points P2 and P3 were located 1.1 m from the panel and the spacing between P1 and P2 and between P3 and P4 was set at 0.3 m in the numerical simulations. The phase and magnitude of the pressures at the four points can be used to formulate the magnitude of the plane wave coefficients for right-traveling (A_i and B_t) and left-traveling (A_r and B_r) waves on both sides of the panel, i.e.,

$$A_i = \frac{\mathrm{i}\left(P_1 \mathrm{e}^{\mathrm{i}kz_2} - P_2 \mathrm{e}^{\mathrm{i}kz_1}\right)}{2\sin\left[k(z_1 - z_2)\right]}, \tag{1}$$

$$A_r = \frac{\mathrm{i}\left(P_2 \mathrm{e}^{-\mathrm{i}kz_1} - P_1 \mathrm{e}^{-\mathrm{i}kz_2}\right)}{2\sin\left[k(z_1 - z_2)\right]}, \tag{2}$$

$$B_t = \frac{\mathrm{i}\left(P_3 \mathrm{e}^{\mathrm{i}kz_4} - P_4 \mathrm{e}^{\mathrm{i}kz_4}\right)}{2\sin\left[k(z_3 - z_4)\right]}, \tag{3}$$

$$B_r = \frac{\mathrm{i}\left(P_4 \mathrm{e}^{-\mathrm{i}kz_3} - P_3 \mathrm{e}^{-\mathrm{i}kz_4}\right)}{2\sin\left[k(z_3 - z_4)\right]}, \tag{4}$$

where z_{1-4} correspond to the locations of the 4 measured pressures and k is the wavenumber, ω/c, with ω being the angular frequency of the sound waves and c the sound speed in air. From these plane wave coefficients, the pressure, P, and velocity, V, on both sides of the panel can be obtained as

$$P_0 = A_i + A_r, \tag{5}$$

$$V_0 = (A_i - A_r)/\rho_a c, \tag{6}$$

$$P_h = B_t \mathrm{e}^{-\mathrm{i}kh} + B_r \mathrm{e}^{\mathrm{i}kh}, \tag{7}$$

$$V_h = \left(B_t \mathrm{e}^{-\mathrm{i}kh} - B_r \mathrm{e}^{\mathrm{i}kh}\right)/\rho_a c, \tag{8}$$

Document downloaded by @DAEL, 2026-11-21 07:36:17 - personal use only

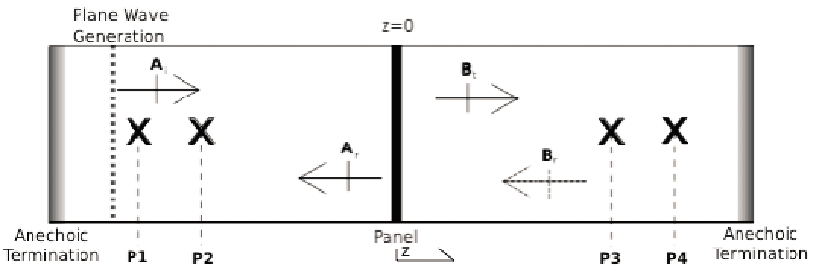


Figure 1. Geometry, measurement points, and defining characteristics of the set up of standing wave tube.

where h is the thickness of the panel and ρ_a is the ambient air density. The subscripts 0 and h here denote the corresponding parameters on the left and right sides of the panel, respectively.

A transfer matrix may be conveniently written to relate the pressure and particle velocity on either side of the panel as

$$\begin{bmatrix} P_0 \\ V_0 \end{bmatrix} = \begin{bmatrix} D_{11} & D_{12} \\ D_{21} & D_{22} \end{bmatrix} \begin{bmatrix} P_h \\ V_h \end{bmatrix}, \tag{9}$$

where the elements of the transfer matrix can be determined according to [16], as

$$\begin{bmatrix} D_{11} & D_{12} \\ D_{21} & D_{22} \end{bmatrix} = \frac{1}{P_0 V_o + P_h V_h} \begin{bmatrix} P_h + P_0 V_0 & P_0^2 - P_h^2 \\ V_0^2 - V_h^2 & P_h V_h + P_0 V_0 \end{bmatrix}. \tag{10}$$

By assuming a unit amplitude incident wave and an anechoic termination at the downstream termination (i.e., $A_i = 1$ and $B_r = 0$), equations (5) to (8) can be simplified to give

$$P_0 = 1 + R, \tag{11}$$

$$V_0 = (1 - R)/\rho_a c, \tag{12}$$

$$P_h = T\mathrm{e}^{-\mathrm{i}kh}, \tag{13}$$

$$V_h = T\mathrm{e}^{-\mathrm{i}kh}/\rho_0 c, \tag{14}$$

where $R = A_r/A_i$ and $T = A_r/A_i$ are the plane wave reflection and transmission coefficients. The transmission coefficient of the panel can then be obtained by substituting equations (11) to (14) into the matrix equation (9) to yield

$$T = \frac{2\mathrm{e}^{\mathrm{i}kh}}{D_{11} + D_{12}/\rho_0 c + \rho_0 c D_{21} + D_{22}}. \tag{15}$$

Hence, the transmission loss (TL) of the panel can be obtained as

$$TL = 10 \log\left(1/|T|^2\right). \tag{16}$$

Before we discuss the sound transmission through a stiffened panel, consider a base model for calculating the transmission loss through a panel with different kinds of elastic supports. In the coordinate system where the tube is oriented along the z-axis, the center of the tube is located at $x = y = 0$ and the tube's width and height are each 1 meter along the x- and y-axes, respectively. The panel was located at $z = 0$, and the model was terminated at $z = 2$ m and $z = -2$ m on each side. The dimensions and material properties used in the control model are listed Table I.

Table I. Relevant dimensions of the single-panel FEM model.

Description of Dimension	Dimension Value
Panel/Tube Height and Width	1 m
Incident and Transmitted Lengths	2 m
Density of Panel	2180 kg/m^3
Young's Modulus of Panel	$68 \cdot 10^9$ N/m^2
Poisson's Ratio of Panel	0.30
Density of Air	1.21 kg/m^3
Speed of Sound in Air	343 m/s
Plane-Wave Generation Location (Upstream of Panel)	1.5 m
Measurement Location of P_1 z_1 (Upstream of Panel), z_1	1.4 m
Measurement Location of P_2 z_2 (Upstream of Panel), z_2	1.1 m
Measurement Location of P_3 (Downstream of Panel), z_3	1.1 m
Measurement Location of P_4 (Downstream of Panel), z_4	1.4 m

While local stiffening of the panel can generate non-plane waves, they do not contribute to the measured pressures since they do not propagate at the frequencies considered here. The non-planar waves create a nearfield close to the panel which may, however, affect the panel natural frequencies through mass loading effects.

The model was formed using two volume elements comprising the upstream and downstream elements of the tube. The model was meshed with a 0.1 m element size in most cases. In the situations that required finer resolution in the panel, a 0.05 m mesh was used. All models were meshed using a mapped square/cubic geometry, where all faces and edges of all elements were of equal-length and at right-angles to each other. At 150 Hz, the wavelength of air is 2.28 m; there would thus be 22 complete elements per wavelength at the highest frequency, thus allowing for adequate resolution in the FEM model.

Document downloaded by @DAEL, 2026-11-21 07:36:17 - personal use only

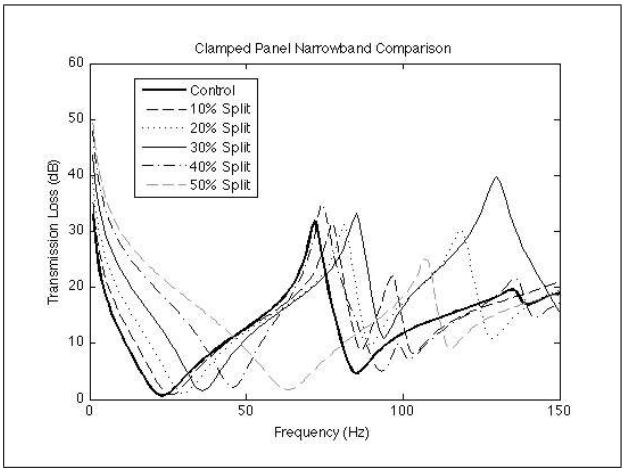


Figure 2. Narrowband transmission loss for select clamped split-panel configurations.

All FEM modeling was implemented in ANSYS [17] using standard element types. In most situations, the simplest possible elements were used to model a particular physical property: unless specified otherwise, similar element types should provide comparable results. The panel was modeled as a shell using the ANSYS SHELL63 element type. Shell elements occupy no space in the geometry of the model, while still accounting for the relevant properties of the panel. The only real constant specified for the shell element was the panel thickness. A damping of 2 percent was assigned to the motion of the panel elements. The shell elements were formed on the faces where the two volumes of the upstream and downstream elements of the tube meet due to ANSYS-imposed restrictions on fluid elements that two adjacent fluid-coupling elements cannot share a face. Thus, the panel consists of two half-thickness plates coupled together (although occupying the same space). This approach creates a response identical to that of a full-thickness plate while conforming to the requirements of the fluid-structure element coupling. For the control model with clamped edge constraints, the points along the edge of the panel were restrained in all degrees of freedom: i.e., neither rotation nor displacement was allowed at the panel edges.

The fluid surrounding the plate was modeled using the ANSYS FLUID 30 element type. The fluid-structure coupling option was used to model the layer of elements nearest to the panel that allows for deformation of the elements. However, no other fluid elements were assigned this coupling option in the ANSYS model. Anechoic ends in the tube were modeled by using a process described by Khan [18] for non-spherical infinite ends. This method allows for nearly anechoic ends on a flat plane so as not to sacrifice the simple structure of the model. In fact, the anechoic ends on both the incident and transmitted sides of the model were created by specifying perfect absorption with the damping factor set at 1.0 in the elements at the inlet and outlet of the model. An impedance flag is also needed at the far end (on the face of the volume) to ensure that ANSYS calculates the energy losses associated with the absorption in the fluid elements.

Plane-wave pressure was generated in the model by specifying a unit pressure degree-of-freedom at all fluid nodes at $z = -1.5$ m. This approach generates waves propagating both towards the panel and towards the far end at the outlet. Anechoic ends were also specified in the ANSYS model to prevent unwanted reflections from the inlet and outlet.

The predicted transmission loss spectrum of the control model is shown as a solid line (marked as control) in Figure 2. The predicted results are shown from 1 Hz to 150 Hz. Beyond 150 Hz (not shown in the figure), the transmission loss follows a generally increasing trend with frequency, as expected from the mass law. However, the clamping of the panel around its edges allows panel modes to occur which can result in decreased transmission loss at the modal natural frequencies.

The modal resonant frequencies of a rectangular panel supported with general boundary conditions are well known [6]. It can be expected that the transmission loss will be reduced near the modal natural frequencies that can couple with the incident sound field. The present model matches theoretical predictions, with the first drop in transmission loss occurring at 23 Hz, which is the frequency of the (1,1) mode of the panel. The next 'dip' in the transmission loss is at 85 Hz, which is just below the 86 Hz (1,3)+(3,1) mode of the panel. The slight decrease in frequency is due to fluid loading on the plate. The third transmission loss minimum occurs near the (3,3) mode of vibration of the panel at 144 Hz.

Only the odd modes of vibration, i.e., those exhibiting a net change in volume, showed reductions in transmission loss. The (2,1) or (2,2) resonance frequencies do not appear, as those modes cannot couple with the incident or transmitted plane waves. While, in principle, the latter behavior will only be seen in a tube structure that limits the incident waves on the panel to normally-incident plane waves, the experimental results presented later in the paper show that this finding is also applicable to random-incidence sound waves at low frequencies.

The peaks in the transmission loss above the first resonant frequency are the result of anti-resonances in the system. The explanation provided by Mulholland [19] is that this behavior is caused by non-transmitting modes of vibration: i.e. modes having no net volume displacement which therefore cannot couple with the incident sound field. It would be possible to use the control model to consider the effect of other general boundary conditions, e.g. simply-supported. However, the findings in those cases are rather similar to earlier work [20] and these results will not be repeated here.

3. The predicted transmission loss of a split window

Several methods were implemented in the model to explore the effects of beam stiffening of a window. Initials tests were performed by clamping the nodes that lie

Document downloaded by @DAEL, 2026-11-21 07:36:17 - personal use only

along a specified location for panel stiffening, as indicated schematically in Figure 3. This represents an ideal constraint to both the translational and rotational response of the panel at the clamped location. Nodes located at 5 percent to 50 percent of the panel height were clamped across the panel in 5 percent height increments; symmetry in the panel dictates that clamping along the width of the panel above 50 percent of the panel will yield identical results to these tests.

Stiffeners were also modeled as beams placed across the panel to simulate a more realistic, non-infinite stiffening of the panel. This was achieved by placing beam elements between the plate nodes at the stiffening locations. The stiffness of the beam was specified by changing the elastic modulus value of the material used in the beam. With a unit moment of area I, a change of the parametric value of Young modulus, E, is equivalent to specifying the bending stiffness, EI, for the beam. The beam was modeled as massless because of the differences in beam construction that would allow for different moments of inertia with different masses.

To simulate elastic edge stiffness, nodes along the edge of the panel were attached to elastic elements; the fixing of those elements to a point in space provides elastic constraint to edge motion. These elastic elements provided both transverse and rotational restraint at the plate edges, but no damping was included in these elements. A uniform stiffness was applied along the entire perimeter of the rectangular panel in each case considered.

The narrowband transmission loss spectra for models clamped at intervals of 10% panel height are shown in Figure 2 together with the predicted results of the control model. Each model exhibits a decrease in transmission loss at the resonance frequency of each section of the panel. The clamping of the panel isolates the vibration between the two segments produced by the split. Each panel segment then exhibits its own resonances in accord with the geometry of the panel segment. A smaller split in the panel causes the panel segments to be of increasingly disparate size, which separates the resonances of each panel segment further. Since each segment is smaller than the unclamped panel, each will have reduced sound transmission at low frequency. When combined with a shift in resonance frequencies, this mechanism will increase the transmission loss. However, at a 50 percent split, each panel has the same resonance, which does not effectively reduce sound transmission. Similar effects occur with other nearly-equal segment sizes (seen in the 40 percent split, for example).

To illustrate this point, the mean transmission loss averaged from 1 Hz to 150 Hz for all stiffening heights is shown in Figure 4. The simulated data show that for the frequency range considered, the 30 percent split provides the best balance between the reduction of individual panel segment sizes and the separation of the resonance frequencies, as evidenced by the high average transmissions loss. Optimization of the panel split height to maximize transmission loss was not performed, but the data would indicate that the ideal split height would be between 25 and 30% of the panel height for the window geometry and frequency range considered here.

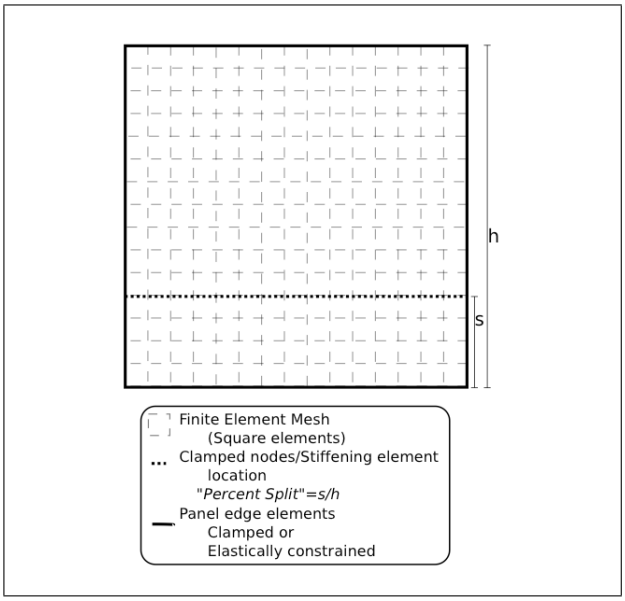


Figure 3. Schematic of finite element mesh show square mesh across panel and clamped node/stiffening element locations.

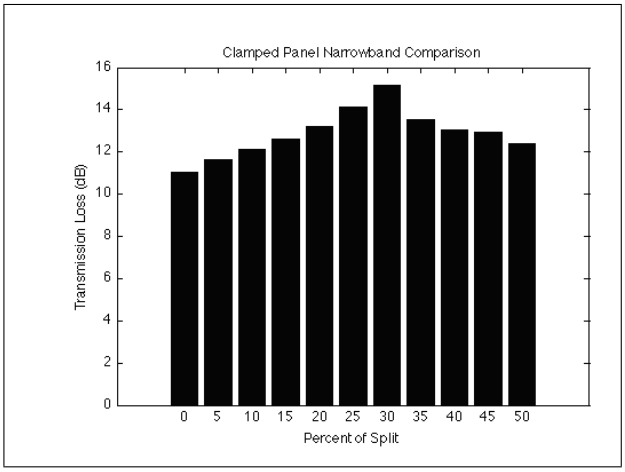


Figure 4. Mean transmission loss averaged from 1 Hz to 150 Hz for clamped, split-panel configurations of a window.

The mean transmission loss results from models with solid stiffening beams across the panels are shown in Figure 5. The abscissa is the bending stiffness (EI) of the stiffening element, while the ordinate is the mean transmission loss from 1 Hz to 150 Hz. The most significant feature in the plot is that a constant transmission loss is reached after a bending stiffness (EI) of 10^4 to 10^5 N m^2 is reached. The exact EI value at which the transmission loss becomes constant is dependent on the height of the stiffening element within the panel. This result indicates that the stiffening effects seen in clamped panels are obtainable at non-infinite values of panel stiffness, even though coupling between the two sections of the panel is present in these cases. Below the transition to a constant

Document downloaded by @DAEL, 2026-11-21 07:36:17 - personal use only

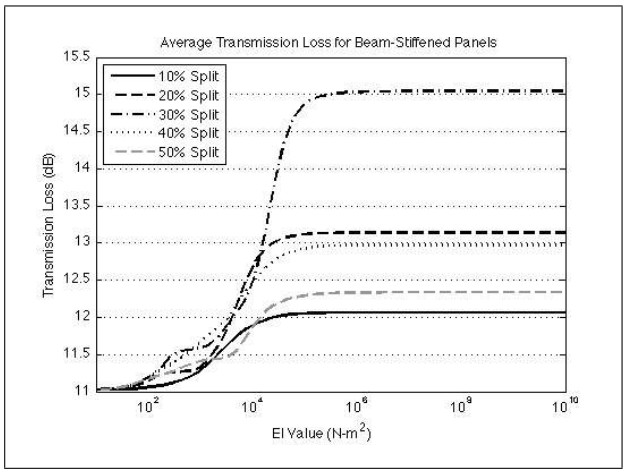


Figure 5. Variation of mean transmission loss with the split height and bending stiffness of the beam.

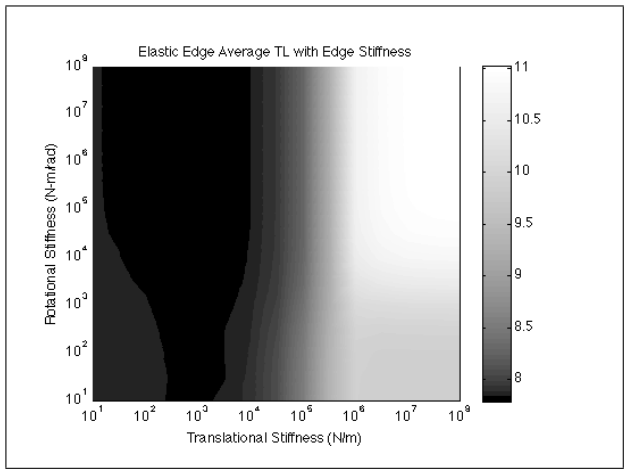


Figure 7. Variation in mean transmission loss with the translational and rotational stiffness for an elastically-mounted panel.

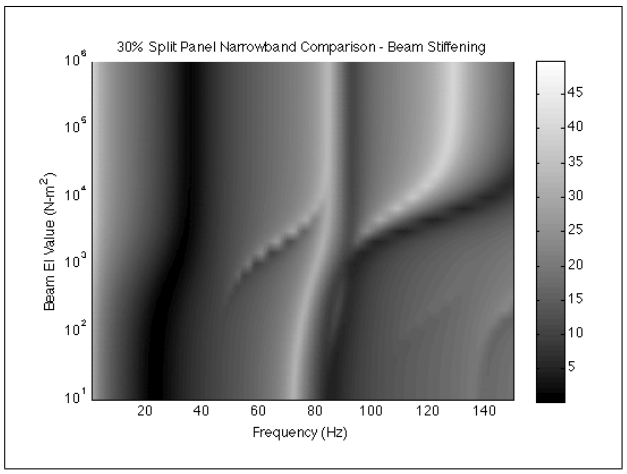


Figure 6. Narrowband transmission loss for beam stiffness with a 30 percent panel split.

transmission loss, each split has its own characteristic, and different splits could be more effective than the 30 percent split at lower stiffnesses. A sample narrowband plot of transmission loss variation with the bending stiffness of the beam for stiffening elements at 30% of the panel height is shown in Figure 6.

The mean transmission losses for elastically-mounted panels are shown in Figure 7. The abscissa is the translational stiffness of the edge and the ordinate is the rotational stiffness around the edges. The mean transmission loss of the elastic edge configurations is nearly constant when the translational stiffness is low. This suggests that plate translational motion has much more effect on transmission of sound through panels than does the rotational motion at the edge. At higher translational stiffnesses when the plate edges are effectively fixed, low rotational stiffness leaves the panel pinned, and increasing the rotational stiffness is similar to applying a clamped condition and increases the transmission loss accordingly. The increase in rotational stiffness will then restrict the motion of the panel to its central region, while the opposite case (high rotational stiffness and low translational stiffness) still allows for high plate translational amplitude. A translational edge stiffness of approximately 10^6 N/m shows the most dramatic effect on average transmission loss. Thus, if the stiffness of the window mounting is too low, the window transmission loss can be reduced by as much as 3 dB compared to a fully clamped support.

4. Experimental results

Previous experimental work on sound transmission through panels has been focused primarily on the effects of window edge-clamping. The addition of damping or restriction of the edge motion has been shown to increase panel transmission loss. Utley and Fletcher [21, 22] performed experimental measurements on windows to gauge the effects of edge conditions on the transmission loss of single and double panel windows. They found that gasketing windows with a high-damping material increased their transmission loss beyond that provided by low-damping gasketing. Quirt [23] performed measurements on single- and double-pane windows to experimentally gauge the effects of various properties on sound transmission. His results showed good comparisons with mass-law predictions except at low frequencies. Both Utley and Quirt's results were presented in third-octave bands down to 80 Hz, obscuring the influence of resonance frequencies on the transmission loss. Xin *et al.* [24] derived analytical expressions for the transmission loss of finite, double panel configurations with either simply-supported or clamped boundary conditions. They ran experimental tests on a similar setup in a custom mounting rig allowing for both conditions. The narrowband results of the analytical model and experimental results for normal sound incidence compared well, but results for oblique incidence did not agree as well.

In order to validate the FEM models described in the last two sections, indoor laboratory experiments were performed on an elastically-mounted panel system. A series of experiments was designed to allow for elastic panel

Document downloaded by @DAEL, 2026-11-21 07:36:17 - personal use only

mounting. Measurements of the sound transmission loss of a rectangular panel with elastic mounting were performed in a reverberation room.

The reverberation room had dimensions of 7.6 m by 6.1 m by 5.5 m and a volume of about 190 m^3 creating an indoor space for diffuse sound fields with a cut-off frequency of about 100 Hz. Transmitted sound pressure was measured outside the reverberation room in a temporary semi-anechoic space composed of three panels of sound-absorbing material surrounding any measurement equipment outside the room. A pair of Altec N1201-8A speakers was positioned near the center of the room to produce the diffuse sound field. The interior pressure was measured using a Brüel and Kjær (B&K) 4189 microphone and B&K 2619 preamp mounted on a boom. The microphone was powered by a B&K 5935 power supply situated outside the room. A General Radio 1390-A Random Noise Generator was used to produce a white noise signal to be supplied to the speakers within the reverberation room. The generator produced a signal from 0 Hz to 20 kHz, which was then band-pass filtered from 20 Hz to 2 kHz by using a Wavetek 852 filter set. The filtered signal was monitored in the data acquisition system. The signal was then amplified by using a SC Audio 1080 Stereo Amplifier and was fed to the speakers inside the reverberation room. A schematic diagram of the experimental setup is shown Figure 8a, and a photograph of the equipment used inside the reverberation room is shown in Figure 8b.

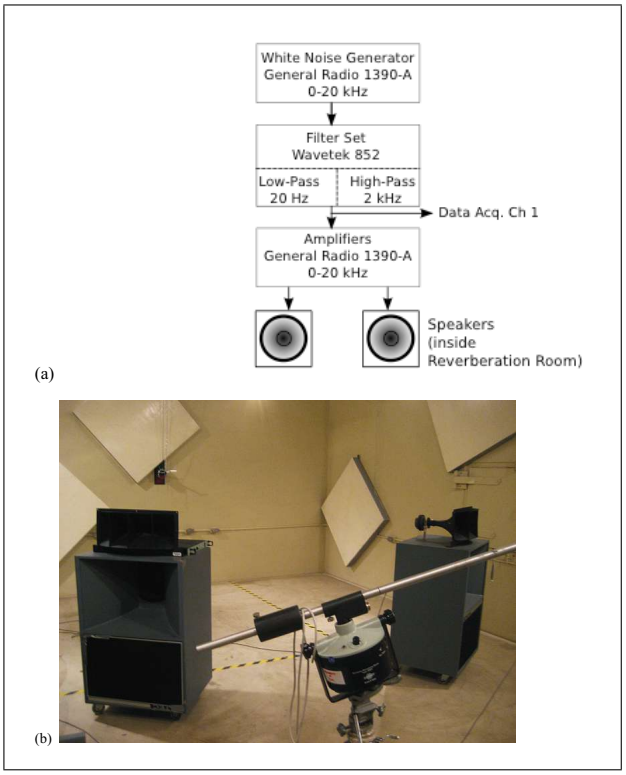


Figure 8. Experimental set up of the study: (a) schematic diagram and (b) photograph of the equipment for noise generation in the reverberation room.

The reverberation room has a square aperture of size 1.21 m by 1.21 m which was designed to hold panels for measurement of sound transmission loss. An adapter was installed in the port in order to allow for testing of the sound transmission specifically associated with lower order modes of a plate. The adapter consisted of a wooden structure filled with sand so as to provide adequate mass to reduce sound transmission through the structure. This arrangement reduces the available aperture dimension down to 27.3 cm square, in which appropriate-sized panels were installed for the experiments. Due to the limitation on the size of the reverberation room and the aperture, and because of relatively high levels of low frequency background noise, accurate results could only be obtained at frequencies above 100 Hz. In the present study, lightweight panels that can be fitted into this port have their first resonant frequency in the range of 180–230 Hz when clamped at their edges.

The panel was mounted in the adapter by using an aluminum frame that screwed directly into the port. Panels to be tested in this configuration were cut to 28.6 cm square to allow for 6.4 mm of the panel material to be clamped between the aluminum frame and the wooden port adapter. Elastic mounting could be achieved by placing lower-density materials such as foam along the 6.4 mm border on both sides of the panel.

A total of seven unique panel configurations were tested. The plate used in all configurations was 2 mm thick aluminum T-6061 alloy. Six different elastic mounting configurations were tested along with a control, clamped-like condition. The variation in each configuration was in the elastic mounting material used around the plate: a total of 6 different mounting stiffnesses were used. The material used for mounting stiffness control was Getzner Sylomer and Sylodyn foams, which are designed for vibration isolation of floor panels or machinery. The Sylodyn foam is a low-damping variation of the Sylomer material, but for the purposes of this experiment only the stiffness properties of the foam were significant. A material thickness of 6 mm was used to provide the resilient edge support.

The measured TL spectra for all the configurations are shown in Figures 9 and 10. Note that the results below 100 Hz should be disregarded since they were entirely determined by background noise levels. The major difference in the TL of each panel configuration occurs near the natural frequencies of the configuration. The sharp decreases in TL occur close to the natural frequencies of the (1,1) and (3,1) modes in each panel configuration: i.e., near 100 Hz and 500 to 600 Hz, respectively. The modes of vibration are more pronounced in the higher-stiffness configurations shown in Figure 10: the (3,1) mode cannot be distinguished in the cases of the two lowest-stiffness foams shown in Figure 9. This could be due to significant damping provided by these foams.

A finite element model was created to simulate the smaller panel size combined with the elastic edge stiffness. The numerical model was similar to that described earlier, but accounted for the smaller size of the experimental setup. The panel thickness and material were adjusted to

Document downloaded by @DAEL, 2026-11-21 07:36:17 - personal use only

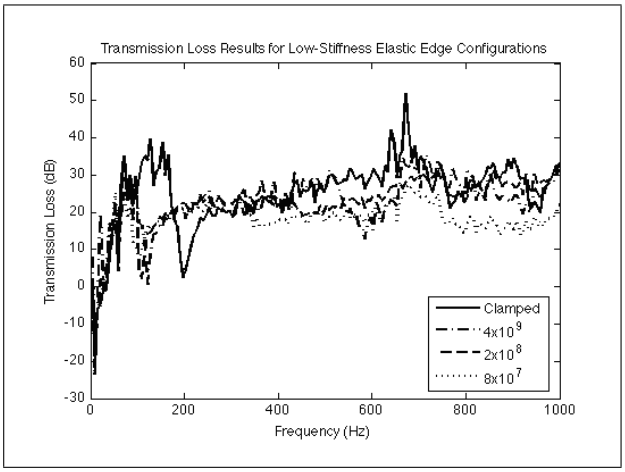


Figure 9. Transmission loss of lower-stiffness elastic mounting conditions. Elastic mounting material stiffness [N/m^2] is given by the manufacturer.

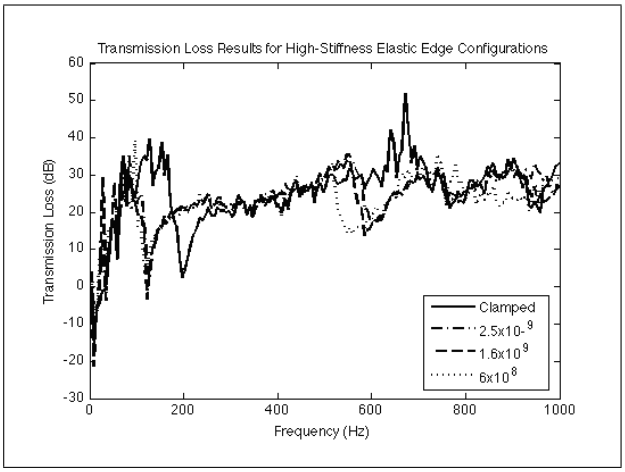


Figure 10. Transmission loss of higher-stiffness elastic mounting conditions. Elastic mounting material stiffness [N/m^2] is given by the manufacturer.

match the panel tested, and all other geometrical parameters were scaled down to maintain a similar geometry with a 0.273 m panel size.

Numerical results from this model were compared with experimentally-obtained results of the transmission loss of the panel. In this analysis, the input translational stiffness was adjusted to provide a best fit between the FEM model results and experimental data. A sample comparison of experimentally-obtained data and TL spectrum calculated using the FEM model is shown in Figure 11.

The predicted results including the elastic edge support fit sufficiently well with the experimental results to verify that the important elements of the TL (in a long duct with anechoic terminations) discussed in section 2 appear in practice for the TL in a reverberation rooms with diffuse sound field. The decrease in TL at the (1,1) and (3,1) natural frequencies is clearly seen in most of the data. The disparity between the fit of the (1,1) peak and the (3,1) peak could be due to mounting inconsistencies; it was found

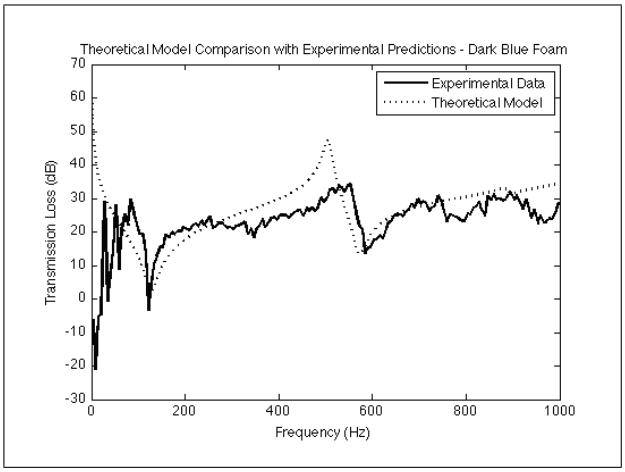


Figure 11. Comparison of experimental data with theoretical predictions for dark blue Sylomer T foam. Estimated material stiffness: $1.6 \cdot 10^9$ N/m^2.

during repetitions of testing that the (3,1) peak is much more sensitive to re-mounting than was the (1,1) peak.

Tests of elastically-mounted panels produced experimental results similar to those predicted by the FEM formulation for a long duct. The odd modes of the panel were observed to transmit the majority of the sound, even under random incidence excitation, though decreased edge stiffness reduced the transmission loss decreases caused by higher-order modes. Finally, the predictions of the FEM model showed a good fit with the experimentally obtained data in the region of the lower natural frequencies of the configuration.

5. Conclusion

Numerical simulations suggest that stiffening elements added to a panel can cause a significant increase in average sound transmission loss at low frequency. The addition of stiffening elements increases the natural frequencies of the modes of vibration of the panel, and in cases of high stiffening, they effectively split the panel into two smaller segments, each of which exhibits modes of vibration at frequencies higher than for the original panel. Thus splitting the panel tends to increase sound transmission loss. However, for splits that yield two panel segments of nearly equal size, this increase was not seen as both panels have high radiation at the same frequency. The FEM model showed that a split at 30 percent of the height of the panel provided the best balance between shifted natural frequencies and reduction of panel size, and gave the highest average transmission loss from 1 Hz to 150 Hz, with an increase of 4 dB from the nonstiffened panel.

The addition of elastic edge mounting to plates reduces the natural frequencies of the panel configuration. In extreme cases, particularly with low rotational stiffness, the mode shapes can change significantly. These changes in mounting stiffness can cause as much as 3 dB decrease in the transmission loss of typical window configurations.

Experimental testing on elastically-mounted panels showed the predicted effects, with lower natural frequen-

Document downloaded by @DAEL, 2026-11-21 07:36:17 - personal use only

cies found in the cases of elastic edge mounting of lower stiffness. The sound transmission at non-resonant frequencies was not dependent on the mounting stiffness, but the resonance of the modes of vibration of the plate caused low transmission loss regions. Numerical simulation results obtained using the FEM model agreed well with experimental results, despite the difference in incident sound field type in the simulation and experiment.

Acknowledgement

The project was supported by the Federal Aviation Administration (FAA) under Contract/Grant Nos. 07-C-NE-PU, and was monitored by Dr. Hua (Bill) He, Office of Environment and Energy of the FAA. The authors gratefully acknowledge the encouragement received from the FAA PARTNER Center of Excellence. Any opinions, findings, and conclusions or recommendations expressed in this material are those of the authors and do not reflect the noise policies of the FAA.

References

[1] Guideline for sound insulation of residences exposed to aircraft operations. US Department of Transport, DOT/FAA/PP-92-5, 1992.

[2] L. L. Beranek (ed.): Noise Reduction. McGraw-Hill, New York, NY, 1947.

[3] E. C. Sewell: Transmission of reverberant sound through a single-leaf partition surrounded by an infinite rigid baffle. Journal of Sound and Vibration **12** (1970) 21–32.

[4] F. G. Leppington: Resonant and non-resonant acoustic properties of elastic panels. Part 2: The transmission problem. Proceedings of the Royal Society of London. Series A, Mathematical and Physical Science **412** (1987) 309–337.

[5] A. W. Leissa: The free vibration of rectangular plates. Journal of Sound and Vibration **31** (1973) 257–293. See also A. W. Leissa: Vibration of Plates, Acoustical Society of America (1993).

[6] K. M. Li, Z. Yu: A simple formula for predicting resonant frequencies of a rectangular plate with uniformly restrained edges. Journal of Sound and Vibration **327** (2009) 254–268.

[7] F. X. Xin, T. J. Lu, C. Q. Chen: Sound transmission through simply supported finite doublepanel partitions with enclosed air cavity. Journal of Vibration and Acoustics **132** (2010) 011008.

[8] D. J. Mead: Wave propagation and natural modes in periodic systems: 1. Mono-coupled systems. Journal of Sound and Vibration **20** (1975) 1–18.

[9] D. J. Mead: Plates with rectangular stiffening in acoustic media: Vibration and radiation. Journal of the Acoustical Society of America **88** (1990) 391–401.

[10] J. H. Lee, J. Kim: Analysis of sound transmission through periodically stiffened panels by space-harmonic expansion method. Journal of Sound and Vibration **251** (2002) 349–366.

[11] J. Wang, T. J. Lu, J. Woodhouse, R. S. Langley, J. Evans: Sound transmission through lightweight double-leaf partitions: theoretical modeling. Journal of Sound and Vibration **286** (2005) 817–847.

[12] D. M. Photiadis: Anderson localization of one-dimensional wave propagation on a fluid loaded plate. Journal of the Acoustical Society of America **91** (1992) 771–780.

[13] Z. Fan: Transient vibration and sound radiation of a rectangular plate with viscoelastic boundary supports. International Journal for Numerical Methods in Engineering **51** (2001) 619–630.

[14] N. Atalla, J. Nicolas, C. Gauthier: Acoustic radiation of an unbaffled vibrating plate with general elastic boundary conditions. Journal of the Acoustical Society of America **99** (1996) 1484–1494.

[15] A. Berry: A general formulation for the sound radiation from rectangular, baffled plates with arbitrary boundary conditions. Journal of the Acoustical Society of America **88** (1990) 2792–2802.

[16] B. H. Song, J. S. Bolton: A transfer-matrix approach for estimating the characteristic impedance and wave numbers of limp and rigid porous materials. Journal of the Acoustical Society of America **107** (2000) 1131–1152.

[17] ANSYS user's manual for revision 10.0. Houston, PA: Swanson Analysis Systems, Inc., 1992.

[18] M. S. Khan, C. Cai, K. C. Hung: Acoustics field and active structural acoustic control modeling in ANSYS. ANSYS International Conference Proceedings, Singapore, 2002.

[19] K. A. Mullholland, R. H. Lyon: Sound insulation at low frequencies. Journal of the Acoustical Society of America **54** (1973) 867–878.

[20] Z. Yu, K. M. Li, D. Y. Ou, C. M. Mak: The effects of fluid loading and elastic supports on the transmission loss of low-frequency noise through single-pane windows. Noise Control Engineering Journal **58** (2010).

[21] W. A. Utley, B. L. Fletcher: Influence of edge conditions on the sound insulation of windows. Applied Acoustics **2** (1969) 131–136.

[22] W. A. Utley, B. L. Fletcher: The effect of edge conditions on the sound insulation of double windows. Journal of Sound and Vibration **26** (1973) 63–72.

[23] J. D. Quirt: Sound transmission through windows. I. Single and doubling glazing. Journal of the Acoustical Society of America **73** (1982) 834–844.

[24] F. X. Xin, T. J. Lu: Analytical and experimental investigation of transmission loss of clamped double panels: implication of boundary effects. Journal of the Acoustical Society of America **125** (2009) 1506–1517.

Document downloaded by @DAEL, 2026-11-21 07:36:17 - personal use only